



Experimental and theoretical analyses of transformation temperatures of Cu-based shape memory alloys

V SAMPATH^{1,*}, SAI VENKATA GAYATHRI² and R SRINITHI¹

¹Department of Metallurgical and Materials Engineering, Chennai 600036, India

²Department of Metallurgical and Materials Engineering, National Institute of Technology, Tiruchirappalli, Trichy 620015, India

*Author for correspondence (vsampath@iitm.ac.in)

MS received 23 November 2018; accepted 11 April 2019

Abstract. Binary-shape memory alloys that are based on copper, mainly copper–aluminium, copper–zinc and copper–tin alloys, either with or without ternary elemental additions, are of special interest to the industry and academia because of their good shape recovery, ease of processing, larger recovery strain and lower cost. However, unlike Ni–Ti shape memory alloys, their uses are moderately limited due to shortcomings, such as stabilization of martensite due to ageing, brittleness and low mechanical strength. Therefore, efforts have been made over the years to overcome these limitations using appropriate ternary and quaternary elemental additions. This work takes into account the data obtained from the experimental work carried out by the authors of this paper as well as the data obtained from the experimental and theoretical works carried out by earlier researchers in this area that have been published in the literature over the years. It is observed in quaternary shape memory alloys based on copper that with an increase in the atomic radius of the quaternary element, the hysteresis width is found to increase. With the addition of ternary elements to binary Cu-based alloys (Cu–Al and Cu–Zn), and quaternary elements to ternary Cu-based alloys (Cu–Al–Fe, Cu–Al–Ni, Cu–Al–Mn, Cu–Zn–Al, Cu–Zn–Ni and Cu–Zn–Si), the M_s temperature either increases or decreases. This influence is directly correlated with the e_v/a ratio and c_v values. It is also observed that as the concentration of electrons decreases, the M_s temperature decreases too. In addition, in this paper, we have tried to obtain relationships between the M_s temperature and the mass or atomic% of different elements through multiple regressions to generalize the interpretations.

Keywords. Shape memory alloys; transformation temperatures; e_v/a ratio; concentration of valence electrons; hysteresis; martensite.

1. Introduction

Shape memory materials are a type of smart materials that have the ability to remember their initial shape before deformation just by heating them above a certain temperature. This behaviour of remembering their earlier shape is called the shape memory effect (SME). It is a functional property, wherein the strain imparted to the material/ally by deformation in the martensitic state ($T < M_f$), i.e., at a lower temperature, is recovered upon heating it to a higher temperature ($T \geq A_f$) [1]. The martensite formed is thermoelastic in nature [2] and the deformation occurs by detwinning the martensite formed on loading. The shape memory effect is also known as thermal memory effect as it is a change in the temperature, i.e., heating, that gives rise to shape recovery. The temperatures at which the phase changes start (M_s , martensite start and A_s , austenite start) to occur and finish (M_f , martensite finish and A_f , austenite finish) leading to a shape change are quite characteristic of the alloy. These transformation temperatures are also called characteristic transformation temperatures since they are highly dependent on the composition of the alloy.

SMA's have captivated the interest of researchers not only because of the SME, but also due to SE, which is also known as the mechanical memory effect. Both SME and SE are used in a wide range of engineering, medical and commercial applications. Devices based on shape memory alloys are used in many engineering, medical and commercial applications [3]. In these applications, the principles of SME and SE are used. These applications are decided by the transformation temperatures of the shape memory alloys that are used to make them. In recent times, there have been studies on SMA's to correlate the transformation temperatures with different experimental and theoretical factors. But, these studies are limited in scope and deal with a few specific shape memory alloy systems. This paper, therefore, discusses in detail the role of e_v/a and c_v , especially in copper-based alloys as no studies have exclusively been carried out on copper-based alloys in detail from these aspects. Apart from the composition, there are also other factors that greatly influence the transformation temperatures, such as grain size, presence of crystal defects, solutionizing temperature, ageing, ordering, etc. In particular, in Cu-based alloys, the degree of order strongly determines the transformation temperatures. Quenching leads to a

higher degree of disorder and thus, lowers transformation temperatures. Short low temperature annealing above A_f can restore the degree of order and thereby increase the transformation temperatures.

A large increase in shape memory behaviour, due to the accumulation of the reversible martensitic deformation, occurs due to the elimination of the permanent (plastic) deformation. In this context, HEAs captivated our interest because of the mechanism of strengthening explains the high strength achieved in terms of change in the Burgers vector along the dislocation line, since its component is perpendicular to the gliding plane. High entropy alloys might also crystallize into an ordered structure like B2 [4]. The austenitic phase in different shape memory intermetallics, especially Ni–Ti SMAs, crystallizes into an ordered B2 structure [5]. The variation in e_v/a from 3 to 10 paralleled to general crystal structure changes, i.e., hcp \rightarrow bcc \rightarrow fcc, in accordance with the literature. From an analysis of the phase transformations in HEAs based on the information available in the paper published by Guo and Liu [6], it is evident that HEA intermetallics with a B2 crystal structure is found in the e_v/a range of around 7. As in conventional SMAs, in HEA also e_v/a plays a critical role.

The martensitic transformation is traditionally considered to have an electronic origin [7]. According to the literature, the hydrostatic pressure and magnetic fields also influence martensite phase formations in SMAs. The change in the M_s temperature increases with an increasing magnetic field strength in both the alloys irrespective of whether they undergo thermoelastic martensitic transformation or not [8]. An earlier work on Ni–Ti SMAs shows a clear dependence of M_s on the e_v/a ratio, i.e., the number of 4s + 3d electrons per atom and c_v [2], in ternary and quaternary Ni–Ti SMAs. The valence electron concentration and e_v/a ratio are highly dependent on the type of ternary and quaternary elemental additions and the amount in which they are added. Although the dependence of transformation temperatures on the e_v/a ratio of Ni–Ti shape memory alloys has been explored earlier [2,9], there has been no published work yet in the public domain correlating the experimental and theoretical factors with the transformation temperatures of SMAs in general and Cu-based SMAs in particular. This work, therefore, served as an impetus for us to delve deeper into the subject.

Cu-Based SMAs evolve from three binary alloy systems: Cu–Al, Cu–Zn and Cu–Sn. Binary Cu–Al SMAs with ternary additions of Fe, Mn and Ni and binary Cu–Zn SMAs with the ternary additions of Ni and Al have been explored in the past for their shape memory properties [10,11]. The martensitic transformation occurring in Cu–Sn shape memory alloys does not result in the formation of a thermoelastic martensite. Moreover, ageing at moderate temperatures results in degradation of shape memory properties. Most of the devices based on SMAs make use of them in the form of wires, sheets, foils, etc. This being the case, the SMAs should be amenable for mechanical processing into these shapes. But, Cu–Sn SMAs are difficult to process into these shapes as the alloys are brittle.

Secondly, most of the Cu–Sn SMAs exhibit their transformation temperatures (M_s , M_f , A_s and A_f) below room temperature. Therefore, the alloys cannot be used in devices that operate about or above room temperature. Thirdly, Cu–Sn SMAs exhibit SME within a very narrow range of compositions [12], thereby, making it difficult to control their compositions during production and also subsequently use them in intended applications. Fourthly, the strain recovery of the alloys is very minimal and their thermal hysteresis is large. As a result, the number of papers that have been published so far is minimal. Moreover, they are of academic interest only and deal with such methods as rapid solidification processing [13]. In this work, therefore, Cu–Sn alloys have not been considered for analysis. Despite their poor mechanical properties as compared to Ni–Ti SMAs, Cu-based SMAs are being explored as a viable substitute to them due to their ease of production and processing [10] and lower cost of production.

2. Materials and methods

Cu–Al–Fe alloys with 12–13 wt% of aluminium and 4 wt% of iron were selected for the present work, as these materials exhibit a β -phase at elevated temperatures and show SME on drastic cooling to room temperature to allow the formation of martensite in this composition range. Small pieces of copper, aluminium and iron of high purity (99.99%) were removed from the respective metal ingots and taken in appropriate amounts, so as to weigh 300 g of the alloy. The pieces were melted in an air induction furnace in the presence of argon. The liquid alloy was decanted into a pre-heated ($\sim 200^\circ\text{C}$) mould measuring $110 \times 60 \times 3$ mm and made of cast iron. The molten alloy was then allowed to solidify. The cast ingots/biscuits were then homogenized by heating to 900°C and holding them at this temperature for 1 h under an argon atmosphere to obtain a completely homogenized alloy that was free from micro-segregation. Quenching of the alloy following homogenization facilitated the formation of martensite in the alloy. Two different compositions were prepared for the present studies. The compositions of the prepared alloys are given below:

- (1) Cu–12Al–4Fe (wt%) {solutionized at 900°C for 1 h}.
- (2) Cu–13Al–4Fe (wt%) {(1) solutionized at 900°C for 1 h, (2) solutionized at 950°C for 1 h}.

The compositions of the alloys were experimentally determined by energy dispersive X-ray (EDAX) analysis. A differential scanning calorimeter (DSC) (NETZSCH-204) was used to measure the transformation temperatures of the prepared alloys. The samples were heated and cooled at a rate of $20^\circ\text{C min}^{-1}$. Specimens with 1 mm thickness and 3 mm diameter were machined from the rolled, solutionized and quenched alloy samples.

3. Factors affecting transformation temperatures

To date, the strong composition dependence of the transformation temperatures, especially, the M_s temperature, has not been fully explored. In recent years, researchers have modified the transformation temperatures as well as the width of the hysteresis by adding appropriate alloying elements to pure elements and to binary and ternary alloys, etc. The selection of the right elemental addition is important if the transformation temperatures are to be increased or decreased. For example, in the case of the ternary addition to binary Ni–Ti alloys, the use of tungsten to replace nickel results in the M_s temperature being raised above room temperature. On the other hand, using tungsten to replace titanium leads to the M_s temperature being lowered to below room temperature [2].

A review of the literature reveals that the M_s temperature depends on the quenching as it drastically lowers the M_s temperature [14]. Martensitic transformation involves lattice transformation without diffusion. Lattice dynamics is therefore considered an important parameter in austenite to martensite transformation. Addition of alloying elements and the presence of lattice defects also have an influence on the lattice dynamics. As per the literature [14], even a change in the composition, as low as 1 at.%, can lead to a change in the elastic constant to the extent of 10%. Quenching, which leads to proliferation of point defects, has a similar effect as well [15]. These contradict the fact that the elastic constants of non-transforming alloys, i.e., those alloys that undergo parent to intermediate phase change, but do not lead to the formation of martensite, are insensitive to alloying and defects [14]. This suggests that martensitic transformation is controlled by lattice dynamics. Lattice dynamics is, therefore, a prerequisite to understand the compositional dependence of M_s .

Apart from the above-mentioned factors, the M_s temperature is also influenced by precipitation, due to ageing effects, point defects, dislocations and ordering. A study of the relevant literature [14] reveals that the transformation temperatures are higher for lower ageing temperatures and lower for higher ageing temperatures. The transformation temperatures remain unchanged even after longer ageing times. This is attributed to the change of matrix composition with indicated solubility limit. Small-sized precipitate particles also tend to decrease the M_s temperature. This is attributed due to the presence of coherency stress.

Ahlers [16] established the role of composition on M_s temperature of ternary Cu–Zn–Al alloys and found that as the Zn content increases, the M_s shifted to lower values by ~ 80 K. Moreover, for ternary Cu–Zn–Al alloys whose e_v/a ratio is 1.48, the high temperature austenite (β) is stable even on slow cooling to room temperature since it is a low temperature phase. In the case of the slowly cooled sample as well as quenched and aged sample, the M_s temperatures obtained were the same so long as the T_Q is lower than $L2_1$ ordering temperature. If not, the reordering that occurs on quenching leads to the retention of small domains that are retained on ageing and lead to a slight change in the M_s temperature, but

in any case, not higher than 4 K. In a binary Cu–Zn system, quenching results in the change of M_s by lower than 7 K, i.e., M_s is not greatly affected. They conclude that in ternary Cu–Zn–Al and binary Cu–Zn alloys, it is possible to control the change in M_s temperature caused by quenching and ageing.

The transformation temperatures are influenced by the solutionizing temperature [17]. It is possible to vary the transformation temperatures of an alloy without changing its composition just by solutionizing the alloy at different temperatures.

3.1 Effect of the e_v/a ratio

The electrons present in the outermost orbitals of an atom are called valence electrons. The e_v values of some of the elements that are used in producing the shape memory alloys are: Cu = 11, Zn = 12, Sn = 4, Fe = 8, Mn = 7, Ni = 10, Cr = 6, Al = 3, Si = 4 and Mg = 2. The e_v/a for an element is calculated as per the following relationship: $e_v/a = \Sigma(\text{at\%} \times e_v)/100$. Accordingly, the e_v/a of any quaternary Cu–X–Y–Z alloy is given by the following equation:

$$e_v/a = f_{\text{Cu}}e_v^{\text{Cu}} + f_Xe_v^X + f_Ye_v^Y + f_Ze_v^Z, \quad (1)$$

where f_{Cu} , f_X , f_Y and f_Z indicate the atomic fractions of Cu, X, Y and Z, respectively, while e_v^{Cu} , e_v^X , e_v^Y and e_v^Z , respectively, indicate the valence electrons present. When the e_v/a ratio is above 7.50, the transformation temperatures show much less dependence on c_v and can be lower than those for alloys with e_v/a between 5 and 7.5. A similar trend is observed even for low and medium c_v values, i.e., 0.17–0.22 [9].

3.2 Effect of valence electron concentration

The average valence electron concentration of an alloy is denoted by c_v (concentration of valence electrons). It is defined as the ratio between the number of valence electrons and the total number of electrons present in the alloy. Mathematically, it can be expressed as:

$$c_v = e_v/e_t, \quad (2)$$

$$c_v = (f_{\text{Cu}}e_v^{\text{Cu}} + f_Xe_v^X + f_Ye_v^Y + f_Ze_v^Z)/(f_{\text{Cu}}Z_{\text{Cu}} + f_XZ_X + f_YZ_Y + f_ZZ_Z), \quad (3)$$

where Z_{Cu} , Z_X , Z_Y and Z_Z represent the atomic numbers of Cu, X, Y and Z, respectively.

In binary Ni–Ti shape memory alloys, the M_s (900 to -100°C) and A_s (950 to -30°C) temperatures decrease as c_v increases (0.1425–0.296) [2], showing a clear correlation between c_v and transformation temperatures. As quoted in the relevant literature, the c_v , M_s and A_s values start increasing when the electron concentration is above 0.34–0.35 [9].

3.3 Effect of transformation hysteresis

As per the literature [18], the thermal hysteresis, $|A_f - M_s|$, which is related to the austenite–martensite interface movement decreases with increasing e_v/a and c_v . The elastic hysteresis, which is related to the energy dissipated because of material’s internal friction, is given by $|A_f - A_s|$. It increases at a slower rate with the valence electron concentration per unit volume.

Hysteresis plays a key role in the selection of shape memory alloys for various applications. Repeated actuation processes, as in SMA actuators, require a smaller hysteresis, whereas vibration damping as in earthquake-resistant structures requires SMAs with a broader hysteresis. Hysteresis is influenced by myriad factors [19], some of which are: (a) atomic radius of the alloying element, (b) lattice compatibility, (c) biasing stress in bimorph and (d) precipitation.

4. Results and discussion

The results of the composition analyses carried out on one of the alloy systems based on copper are shown in figure 1a and b.

The calculated e_v/a and c_v values on experimentally determined austenite–martensite and martensite–austenite transformation temperatures of ternary, quaternary and quinary Cu-based SMAs based on the work [20,21] of one of the authors (V Sampath) of the paper and other researchers are given in tables 1–3.

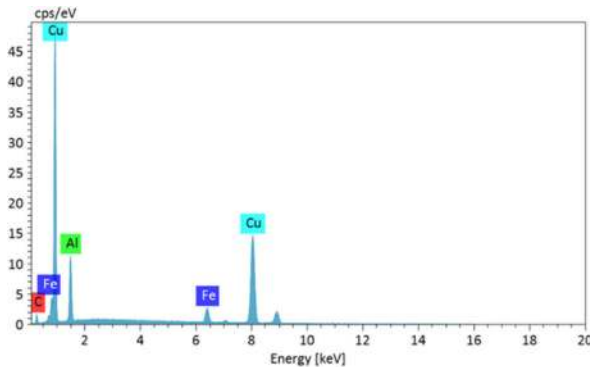
Regression analysis: The regression equation for the dependence of M_s on the alloying elements (composition) in Cu–Al alloys is derived using the Minitab software. The statistical data from regression analysis were obtained as follows: $S = 38.3851$; $R\text{-Sq} = 87.96\%$ and $R\text{-Sq}(\text{adj}) = 81.93\%$.

Regression equations for the Cu–Al system:

$$M_s (\text{°C}) = 706 - 32.3Al - 20.7Fe + 41.5Mn - 26.3Ni. \tag{4}$$

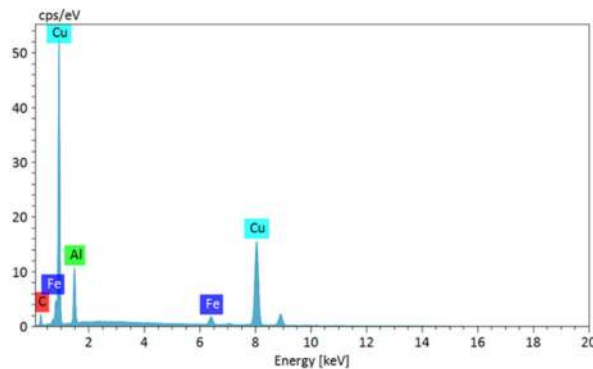
The dependence of M_s on e_v/a was also obtained in a similar fashion for Cu–Al alloys. Statistical data from regression analysis were obtained as follows: $S = 94.2735$; $R\text{-Sq} = 0.11\%$ and $R\text{-Sq}(\text{adj}) = 0.00\%$.

$$M_s (\text{°C}) = 179 + 7.2e_v/a. \tag{5}$$



(a) Composition of Cu-12Al-4Fe alloy

Element	At. No	Wt. %	At. %
Carbon	6	3.47	0.79
Aluminium	13	12.25	6.1
Iron	26	4.67	4.6
Copper	29	79.61	88.45



(b) Composition of Cu-13Al-4Fe alloy

Element	At. No	Wt. %	At. %
Carbon	6	2.07	0.47
Aluminium	13	13.56	6.7
Iron	26	4.39	4.35
Copper	29	79.98	88.48

Figure 1. EDAX results of the Cu–Al–Fe system used in the present study. (a) Composition of the Cu–12Al–4Fe alloy and (b) composition of the Cu–13Al–4Fe alloy.

Table 1. e_v/a , c_v , M_s , M_f , A_s and A_f of ternary, quaternary and quinary Cu–Al-based SMAs.

Alloy	wt% (at%)	e_v/a ratio	c_v	Transformation temperatures (°C)				Ref.	
				M_f	M_s	A_s	A_f		
Cu–Al–Fe	Cu10.21Al4.60Fe (Cu _{91.04} Al _{4.63} Fe _{4.32})	10.49	0.3729	243	308	416	478	[22]	
	Cu11.17Al4.42Fe (Cu _{90.73} Al _{5.09} Fe _{4.17})	10.46	0.3728	232	255	395	450		
	Cu11.56Al4.58Fe (Cu _{90.37} Al _{5.29} Fe _{4.34})	10.45	0.3729	203	232	311	371		
	Cu11.91Al4.62Fe (Cu _{90.05} Al _{5.80} Fe _{4.15})	10.41	0.3725	171	203	200	227		
	Cu12.57Al2.60Fe (Cu _{91.73} Al _{5.81} Fe _{2.48})	10.46	0.3735	181	266	410	445		
	Cu12.58Al1.32Fe (Cu _{92.98} Al _{5.77} Fe _{1.25})	10.50	0.3745	240	250	288	372		
	Cu12.60Al2.11Fe (Cu _{92.21} Al _{5.78} Fe _{2.0})	10.47	0.3738	192	259	399	447		
	Cu12.60Al4.35Fe (Cu _{90.18} Al _{5.63} Fe _{4.37})	10.43	0.3722	114	135	131	160		
	Cu–12Al–4Fe (Cu _{79.61} Al _{12.25} Fe _{4.67})	9.49	0.3665	195	224	408	477	This study	
	Cu–13Al–4Fe (1) (Cu _{79.98} Al _{13.56} Fe _{4.39})	9.54	0.3655	193	249	401	482		
	Cu–13Al–4Fe (2) (Cu _{79.98} Al _{13.56} Fe _{4.39})	9.54	0.3655	174	247	409	485		
	Cu–Al–Mn	Cu12.5Al5Mn (Cu _{89.5} Al _{5.76} Mn _{4.69})	10.35	0.3710	460	510	490	520	[23]
		Cu12.5Al5Mn2Zn (Cu _{87.04} Al _{5.74} Mn _{5.0} Zn _{2.2})	10.29	0.3687	460	500	480	510	
		Cu12.5Al5Mn2Si (Cu _{88.16} Al _{5.81} Mn _{5.06} Si _{0.9})	10.41	0.3737	475	505	490	510	
		Cu12.5Al5Mn2Mg (Cu _{88.27} Al _{5.82} Mn _{5.07} Mg _{0.83})	10.41	0.3753	525	540	260	335	
Cu12.5Al5Mn2Cr (Cu _{87.44} Al _{5.77} Mn _{5.02} Cr _{1.78})		10.40	0.3742	470	490	460	500		
Cu–Al–Ni		Cu12.96Al4.27Ni (Cu _{89.82} Al _{5.98} Ni _{4.29})	10.48	0.3736	—	149	—	—	Obtained using eq. [24]
		Cu13.15Al3.25Ni (Cu _{90.69} Al _{6.08} Ni _{3.26})	10.48	0.3742	—	137	—	—	
	Cu13.5Al4Ni (Cu _{82.5} Al _{6.24} Ni _{4.02})	10.46	0.4045	—	62	—	—	[24]	
	Cu13.7Al4Ni (Cu _{89.63} Al _{6.34} Ni _{4.03})	10.45	0.3739	—	28	—	—		
	Cu13.8Al4Ni (Cu _{89.59} Al _{6.39} Ni _{4.03})	10.45	0.3740	—	11	—	—		
	Cu14Al4Ni (Cu _{89.48} Al _{6.49} Ni _{4.03})	10.40	0.3725	—	–22	—	—		
	Cu–Al–Ni–V	Cu13.0Al4.0Ni0V (Cu _{90.01} Al _{5.99} Ni _{4.0} V ₀)	10.48	0.3743	210	229	325	377	[25]
Cu13.0Al4.0Ni0.5V (Cu _{89.11} Al _{5.99} Ni _{4.02} V _{0.87})		10.42	0.3729	90	111	169	179		
Cu13.0Al4.0Ni1.0V (Cu _{89.56} Al _{5.99} Ni _{4.0} V _{0.44})		10.45	0.3736	180	198	218	227		
Cu13.0Al4.0Ni2.0V (Cu _{88.20} Al _{6.01} Ni _{4.02} V _{1.75})		11.17	0.4007	144	159	196	205		

Table 1. (continued)

Alloy	wt% (at%)	e_v/a ratio	c_v	Transformation temperatures (°C)				Ref.
				M_f	M_s	A_s	A_f	
Cu–Al–Zn–Mn–Si	Cu9.1Al17.1Zn3.0Mn1.1Si (Cu _{83.05} Al _{4.60} Zn _{8.69} Mn _{3.09} Si _{0.58})	10.56	0.3752	1	16	11	30	[26]
	Cu9.0Al17.2Zn3.4Mn0.9Si (Cu _{84.5} Al _{4.06} Zn _{7.87} Mn _{3.13} Si _{0.42})	10.60	0.3754	−18	12	−3	20	
	Cu9.5Al17.1Zn4.2Mn1.0Si (Cu _{83.32} Al _{4.31} Zn _{7.80} Mn _{3.88} Si _{0.47})	10.52	0.3744	−42	−4	−35	8	
	Cu8.7Al16.9Zn3.7Mn0.9Si (Cu _{84.72} Al _{3.92} Zn _{7.31} Mn _{3.40} Si _{0.42})	10.57	0.3751	−26	3	−10	12	
	Cu8.9Al16.7Zn3.7Mn0.9Si (Cu _{84.83} Al _{4.02} Zn _{7.33} Mn _{3.4} Si _{0.42})	10.59	0.3751	−34	2	−20	6	
	Cu8.9Al16.7Zn3.7Mn1.1Si (Cu _{84.72} Al ₄ Zn _{7.34} Mn _{3.4} Si _{0.52})	10.58	0.3750	−31	4	−11	48	
	Cu8.8Al17.7Zn3.2Mn1.1Si (Cu _{84.16} Al _{3.97} Zn _{8.42} Mn _{2.94} Si _{0.5})	10.61	0.3755	−19	8	−5	15	
	Cu8.7Al17.2Zn3.5Mn1.1Si (Cu _{84.47} Al _{3.93} Zn _{7.87} Mn _{3.22} Si _{0.52})	10.60	0.3753	−10	16	1	26	

Numbers within square brackets refers to the sources of transformation temperatures.

Table 2. e_v/a , c_v , M_s , M_f , A_s and A_f of ternary, quaternary and quinary Cu–Zn and Cu–Sn-based SMAs.

Alloy	wt% (at%)	e_v/a ratio	c_v	Transformation temperatures (°C)				Ref.
				M_f	M_s	A_s	A_f	
Cu–Zn–Ni	Cu–45.26Zn–5.47Ni (Cu _{48.84} Zn _{46.12} Ni _{5.01})	11.40	0.3877	74	90	95	138	[27]
	Cu–45.59Zn–5.82Ni (Cu _{48.12} Zn _{46.54} Ni _{5.34})	11.41	0.3879	82	106	105	145	
	Cu–45.63Zn–6.15Ni (Cu _{47.80} Zn _{46.57} Ni _{5.63})	11.40	0.3876	88	112	116	152	
	Cu–46.12Zn–6.21Ni (Cu _{47.25} Zn _{47.06} Ni _{5.69})	11.41	0.3879	108	115	118	143	
	Cu–48.04Zn–2.96Ni (Cu _{48.40} Zn _{48.89} Ni _{2.72})	11.46	0.3889	86	111	101	126	
	Cu–46.86Zn–3.75Ni (Cu _{48.78} Zn _{47.79} Ni _{3.43})	11.44	0.3885	72	121	116	143	
	Cu–45.91Zn–4.47Ni (Cu _{48.95} Zn _{46.95} Ni _{4.10})	11.40	0.3874	66	132	126	156	
Cu–Zn–Al	Cu–25.52Zn–3.74Al (Cu _{71.76} Zn _{26.63} Al _{1.61})	11.13	0.3868	—	50	—	—	[28]
	Cu–26.08Zn–3.85Al (Cu _{71.21} Zn _{27.24} Al _{1.61})	11.15	0.3848	—	−10	—	—	
Cu–Zn–Al–Mn–Ni	Cu–23.6Zn–4.47Al–0.23Mn–0.17Ni (Cu _{72.94} Zn _{24.76} Al _{1.94} Mn _{0.203} Ni _{0.160})	11.08	0.3830	22	39	5	3	[29]
Cu–Zn–Al–Fe	Cu–14.86Zn–5.81Al–0.5Fe (Cu _{81.5} Zn _{15.76} Al _{2.54} Fe _{0.45})	10.94	0.3797	80	111	108	134	[30]
Cu–Zn–Si	Cu–33.4Zn–2.2Si (Cu _{63.66} Zn _{35.34} Si _{1.00})	11.28	0.3855	−10	10	10	50	[31]
	Cu–35.9Zn–1.4Si (Cu _{62.54} Zn _{36.84} Si _{0.62})	11.55	0.3945	−70	−55	−50	−15	
	Cu–33.4Zn–2.1Si (Cu _{64.64} Zn _{34.43} Si _{0.93})	11.28	0.3862	−5	15	15	55	
	Cu35.8Zn1.4Si (Cu _{62.79} Zn _{36.59} Si _{0.61})	11.32	0.3867	−75	−50	−45	−10	
	Cu–30.7Zn–4.3Si (Cu _{65.99} Zn _{32.07} Si _{1.93})	11.18	0.3851	—	−23	—	—	[32]
Cu–29Zn–5Si (Cu _{67.32} Zn _{30.43} Si _{2.25})	11.15	0.3849	—	−10	—	—		
Cu–15Sn	Cu–24.7Sn (Cu ₈₅ Sn ₁₅)	9.26	0.271	−70	−51	90	113	[33]

Numbers within square brackets refer to the sources of transformation temperatures.

The regression equation for the dependence of M_s on the alloying element in Cu–Zn alloys is also derived using Minitab software. Statistical data from regression analysis were obtained as follows: $S = 31.2833$; $R\text{-Sq} = 84.85\%$; $R\text{-Sq}(\text{adj}) = 78.79\%$ and $R\text{-Sq}(\text{Pred}) = 63.99\%$.

Regression equations for the Cu–Zn system:

$$M_s (\text{°C}) = -417 + 10.40\text{Zn} + 9.51\text{Ni} + 44.4\text{Al} + 20.8\text{Si}. \quad (6)$$

Table 3. Hysteresis $|A_f - M_s|$ and atomic radius of alloying element added to ternary, quaternary and quinary Cu-based SMAs [18].

Atomic radius of alloying elements (pm)	Hysteresis (°C)	Composition (wt%)
173 (Mg)	205	Cu-12.5Al-5Mn-2Mg
111 (Si)	5	Cu-12.5Al-5Mn-2Si
128 (Cr)	10	Cu-12.5Al-5Mn-2Cr
139 (Zn)	10	Cu-12.5Al-5Mn-2Zn

The values were taken from table 2.

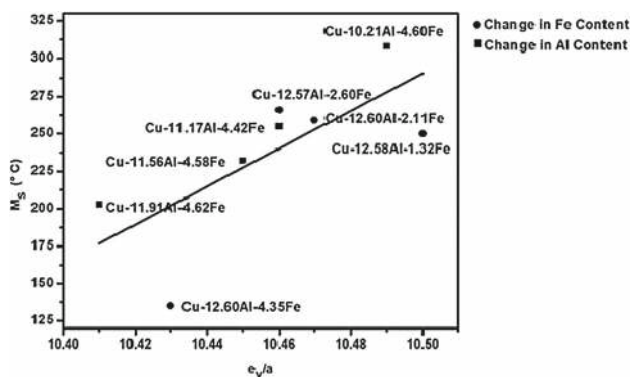


Figure 2. Dependence of M_s on the composition and e_v/a ratio for Cu-Al-Fe SMAs.

The dependence of M_s and e_v/a was also obtained in a similar way for Cu-Zn alloys. The Statistical data from regression analysis were obtained as follows: $S = 63.8252$; $R-Sq = 18.00\%$ and $R-Sq(adj) = 11.69\%$.

$$M_s (\text{°C}) = 2460 + 221e_v/a. \tag{7}$$

Due to the availability of very few compositions on Cu-Sn alloys, no regression analysis was carried out for the same. We have checked the validity of equations (4-7) with regard to correlation between the composition and transformation temperature (M_s) in the case of the experimentally studied alloys and theoretically proposed compositions of the shape memory alloys by the earlier researchers and our own experimental compositions and findings, we observed that the equations have an accuracy of 95%.

In Cu-Al-Fe SMAs, it can be observed (figure 2 and equation (4)) that as the aluminium content increases, the e_v/a ratio decreases and thereby decreasing the M_s temperature as well. From the regression equation also, it can be clearly predicted that with an increase in the aluminium weight percent, there is a decrease in M_s . A similar trend can be observed with increasing iron contents as well, with the exception of Cu-12.58Al-2.60Fe alloy. A higher M_s temperature is generally attributed to the completely filled d-d overlapping orbitals. Such a tendency was observed even in Ni-Ti-X (Pt) alloys,

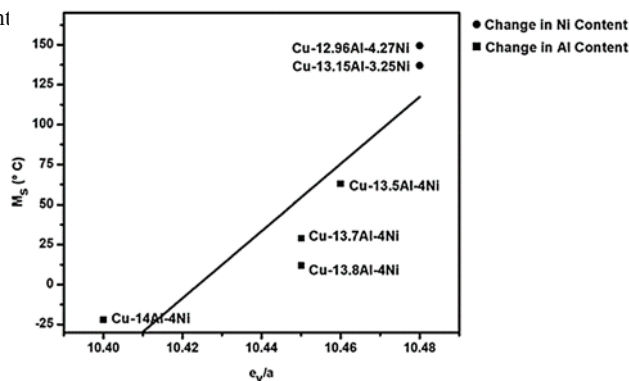


Figure 3. Dependence of M_s on the composition and e_v/a ratio for Cu-Al-Ni SMAs.

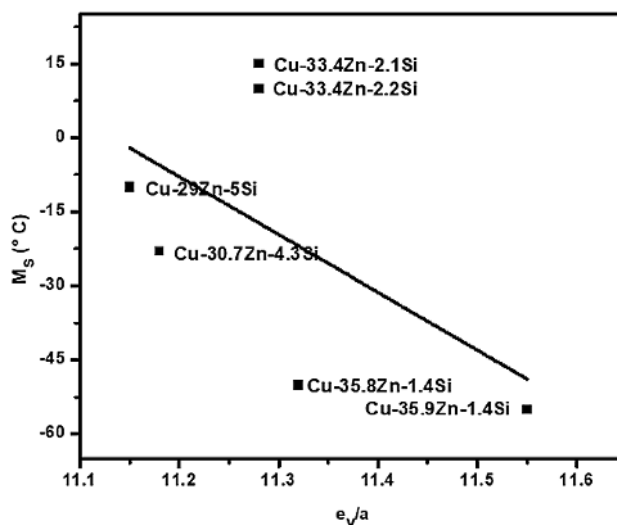


Figure 4. Dependence of M_s on the composition and e_v/a ratio for Cu-Zn-Si SMAs.

exhibiting a broad range of transformation temperatures, with their M_s and A_s as high as 900 and 950°C, respectively, for an e_v/a ratio of 7 [2]. Thus, a clear correlation between the d-d overlapping orbitals in the alloy and the transformation temperature (M_s) can be established.

With a slight increase in the nickel content (1 wt%), as also with a marginal decrease in the aluminium content (0.1 wt%), it can be observed in figure 3 that M_s increases or decreases for the same value of e_v/a . This ratio is constant for the alloys possessing a high M_s temperature (150°C). Even in Cu-Al-Ni SMAs, it can be observed that an increase in the aluminium content as low as 0.1 wt%, drastically decreases the M_s temperature.

Figure 4 reveals that with the silicon and copper contents of the alloys almost remaining constant, even a 0.1 wt% increase in the zinc content tends to reduce the M_s temperature by about 5°C. A similar trend can be observed with an increase in the silicon content also. For almost the same

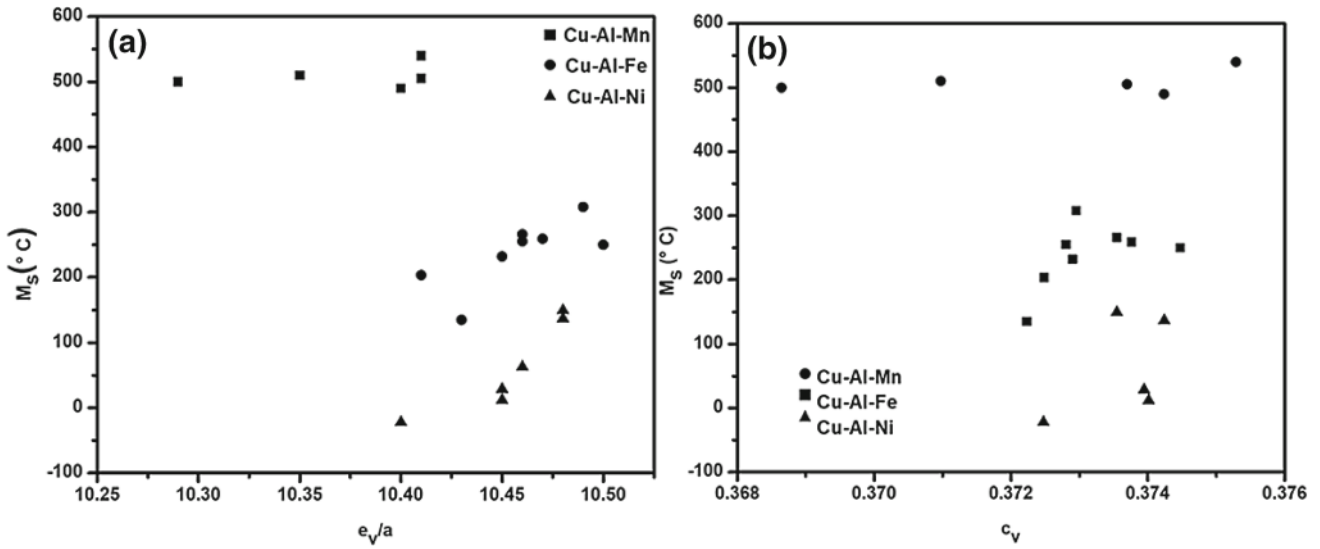


Figure 5. Dependence of M_s of Cu–Al ternary systems [22–24] on: (a) e_v/a ratio and (b) c_v .

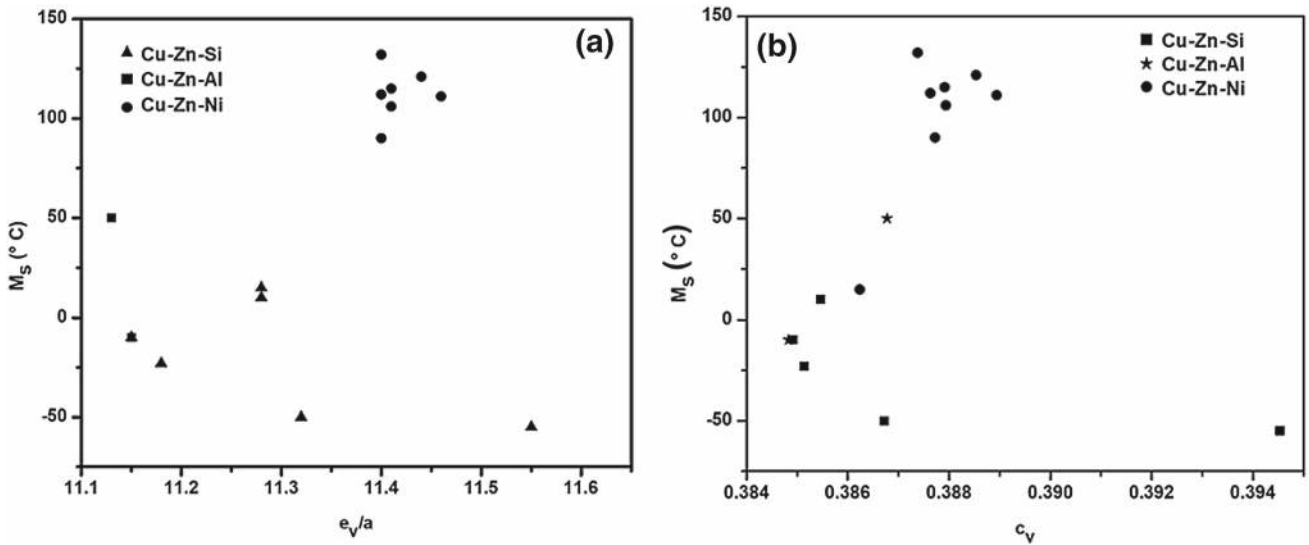


Figure 6. Dependence of M_s of Cu–Zn ternary systems [27,28,31,32] on: (a) e_v/a ratio and (b) c_v .

zinc and copper contents, an increase in the silicon content of 0.1 wt% decreases the M_s temperature by $\sim 5^\circ\text{C}$. As far as the alloy system Cu–Zn–Si is concerned not too many researchers have worked on them over the years. Consequently, not too many data are available on the transformation temperatures of these ternary alloys. Due to the paucity of data, a closer fit could not be obtained.

Every element has a definite atomic number, which influences the transformation temperatures in some specific ways. Plots have therefore been drawn so as to bring out the effect more clearly. The correlation between the M_s temperature and the e_v/a ratio for Cu–Al ternary alloys of different compositions is clearly shown in figure 5a. As can be seen,

many alloys (10 out of 15 of them) have their e_v/a ratios between 10.4 and 10.5. In addition, it can be seen that the highest M_s temperatures (5 out of 15 alloys) are observed in the range of 10.30–10.35.

In the case of M_s vs. c_v correlation (figure 5b), it can be found that the c_v ratio lies in the range of 0.368–0.376 with most of them centred around the values of 0.372–0.375.

As can be seen, the sensitivity of the transformation temperature to c_v is reduced. With increasing valence electrons, the bond strength and hence elastic properties increase even for medium values of c_v . This is attributed to the fact that a higher number of valence electrons leads to a stronger bonding for larger ion kernels in metallic bonds [9]. An increase in

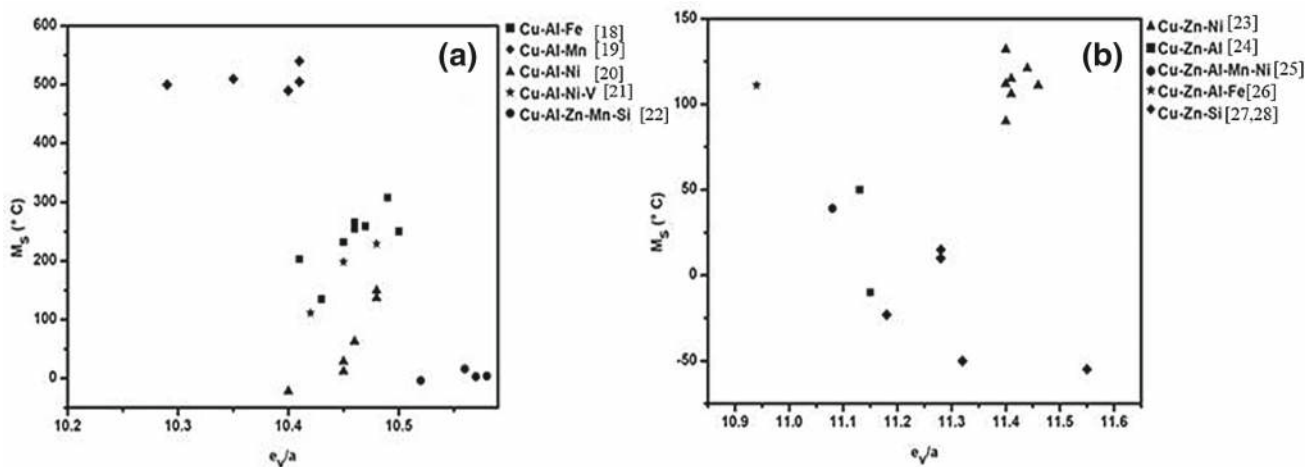


Figure 7. Dependence of M_s on the e_v/a ratio of (a) Cu–Al and (b) Cu–Zn systems.

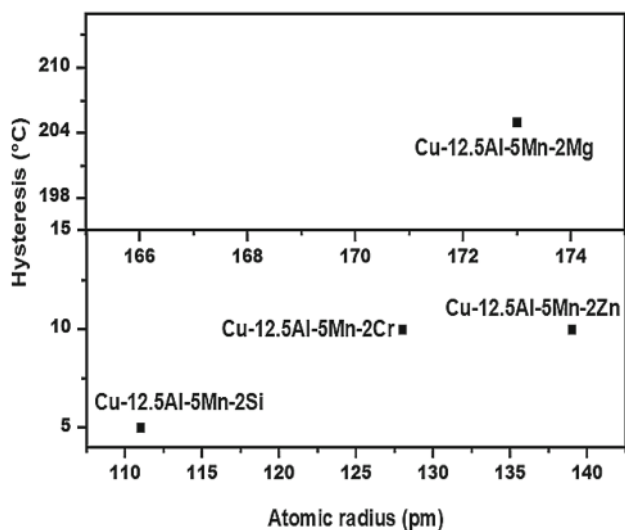


Figure 8. Dependence of hysteresis on the atomic radius of alloying elements.

the e_v/a ratio also leads to decreased M_s temperatures with some degree of deviation from the main trend.

In metals, the behaviour of valence electrons resembles that of a ‘glue’ bringing together the non-valence electrons and the nuclei [9], while the non-valence electrons form the total volume of the alloy. A slight increase in the transformation temperature is observed for $c_v > 0.34$ – 0.35 [9]. This is attributed to the phenomena of anti-bonding and thickening of the ‘glue’ caused by a high concentration of valence electrons as evidenced by the plots.

Alloying is mainly done so as to cause improvement in mechanical (e.g., tensile strength, elastic modulus and ductility) and functional properties (e.g., SME and superelasticity).

As reported in the literature, the change in transition temperatures is attributed to the variation in the bulk elastic modulus of austenite. If the modulus of elasticity of austenite is larger, the alloy should be cooled to lower or sub-zero temperatures before a critical value of the elastic modulus (c_0 , basal-plane shear modulus and c_{44} , monoclinic shear modulus), which may lead to decreased M_s .

The correlation between the M_s temperatures and e_v/a ratios of the ternary alloys based on Cu–Zn is plotted in figure 6a. As can be observed, most of the alloys (11 out of 15) have their e_v/a ratio between ~ 11.25 and 11.5 . It can also be observed that the highest M_s temperatures are observed for the Cu–Zn–Ni system with their e_v/a ratio between 11.40 and 11.46 .

As far as the correlation between M_s and c_v , from figure 6b, it is found that most of the c_v values lie in the range of 0.384 – 0.39 with a majority of them (14 out of 15) hovering around the values in the region of 0.387 – 0.39 . The trend of increasing M_s with increasing c_v can be found.

The valence electron concentration per unit volume (VED) also has a strong influence on the transformation temperature, namely, the M_s temperature [18]. This is because as VED becomes larger, it leads to an increasing modulus, leading in turn to a decreased transformation temperature. This is also the reason as to why M_s decreases as c_v decreases. The higher the number of electrons involved, the stronger are the bonds, and higher are the melting temperatures.

An attempt is made to compare the influence of the e_v/a ratio on the M_s temperature among Cu–Al and Cu–Zn ternary, quaternary and quinary alloys. The trend observed is plotted in figure 7a and b. From figure 7a, we can observe that most of the alloys (20 out of 26) have their M_s hovering between 10.4 and 10.5 . It is also observed that the highest value of M_s is found for the alloy with an e_v/a ratio of 10.4 . From figure 7b, it can be found that most of the alloys (10 out of 16) show their M_s values in the range of 11.25 – 11.50 . It is

also observed that the highest value of M_s is found for the alloy with an e_v/a ratio of 11.4.

The effect of the atomic radius of alloying elements in an alloy having approximately the same e_v/a ratio on hysteresis is illustrated in figure 8. In Mn-rich alloys, it can be observed that the anti-ferromagnetic properties [9] of the alloy lead to higher M_s temperatures.

It is also found that increasing the atomic radius, increases the hysteresis. As can be found in the literature, hysteresis is attributed to two energy dissipation processes during transformation: one is associated with the resistance of the intermetallic bonds, while the other with volume changes and rearrangement. Thus, a higher atomic radius increases energy dissipation, leading to a larger hysteresis.

5. Conclusions

The transformation temperatures of shape memory alloys are very important since their applications in specific fields depend on their stability with time and magnitude. A number of factors influence the transformation temperatures. The present work is an attempt to analyse factors that influence transformation temperatures. This work takes into account the data obtained from the experimental work carried out by V Sampath and his co-workers and also those from the experimental and theoretical analyses carried out by other researchers on copper-based alloys. The work is by no means exhaustive and is rather limited in scope. More detailed experimental and theoretical analyses are required to get a thorough understanding of the subject. However, the following conclusions can be drawn from the experimental and theoretical analyses.

It can be concluded from the obtained correlations that the e_v/a ratio and c_v values play an important role in influencing the M_s temperature. The specific conclusions drawn from the analyses are given below:

- (1) The addition of alloying elements, such as aluminium, iron, zinc and silicon, decreases the e_v/a ratio and thereby decreases the M_s temperature.
- (2) As is the case with Ni–Ti alloys, it is found that c_v influences the martensitic transformation temperature. As c_v decreases, the M_s temperature decreases as well.
- (3) The atomic size/diameter of the elements added determines the hysteresis width. As the atomic radius increases, there is a slight increase in the hysteresis width in most of the quaternary alloys even though there is an exception to this trend.

Acknowledgements

Prof V Sampath and his co-authors are grateful to Prof Jan Van Humbeeck, formerly with Catholic University, Leuven

(KU Leuven), Belgium, for having taken the time to go through the entire manuscript so meticulously and offering very useful, constructive and relevant comments and suggestions for improving the quality of the manuscript. Prof V Sampath gratefully acknowledges the financial support from DST (project no. DST/INT/RUS/RFBFR/P-251) and SERB (project no. EEQ/2016/000500/).

Appendix

In the case of Cu-based shape memory alloys, the electronic configurations of the elements that are added to form the alloys are given by:

Alloy	Atomic number	Electronic configuration
Cu	29	$1s^2 2s^2 2p^6 3s^2 3p^6 4s^1 3d^{10}$
Zn	30	$1s^2 2s^2 2p^6 3s^2 3p^6 4s^2 3d^{10}$
Sn	50	$1s^2 2s^2 2p^6 3s^2 3p^6 4s^2 3d^{10} 4p^6 5s^2 4d^{10} 5p^2$
Fe	26	$1s^2 2s^2 2p^6 3s^2 3p^6 4s^2 3d^6$
Mn	25	$1s^2 2s^2 2p^6 3s^2 3p^6 4s^2 3d^5$
Ni	28	$1s^2 2s^2 2p^6 3s^2 3p^6 4s^2 3d^8$
Cr	24	$1s^2 2s^2 2p^6 3s^2 3p^6 4s^2 3d^4$
Al	13	$1s^2 2s^2 2p^6 3s^2 3p^1$
Si	14	$1s^2 2s^2 2p^6 3s^2 3p^2$
Mg	12	$1s^2 2s^2 2p^6 3s^2$

References

- [1] Wayman C M 1993 *MRS Bull.* **18** 49
- [2] Zarinejad M and Liu Y 2008 *Adv. Funct. Mater.* **18** 1
- [3] Jani J M, Leary M, Subic A and Gibson M A 2014 *Mater. Des.* **56** 1078
- [4] Firstov G S, Kosorukova T A, Koval Yu N and Odnosum V V 2015 *Mater. Today Proc.* **2S** S499
- [5] Otsuka K and Ren X 1999 *Intermetallics* **7** 511
- [6] Guo S and Liu C T 2011 *Prog. Nat. Sci. Mater.* **21** 433
- [7] Huisman-Kleinherenbrink P M, Jian Y and Beyer J 1991 *Mater. Lett.* **11** 145
- [8] Kakeshita T, Fukuda T, Sakamoto T, Takeuchi T, Kindo K, Endo S *et al* 2002 *Mater. Trans.* **43** 887
- [9] Zarinejad M and Liu Y 2008 *Adv. Funct. Mater.* **18** 2789
- [10] Alaneme K K and Okotete E A 2016 *Eng. Sci. Technol.* **19** 1582
- [11] Dasgupta R 2014 *J. Mater. Res.* **29** 1681
- [12] Miura S, Morita Y and Nakanishi N 1975 in *Shape memory effects in alloys* J Perkins (ed) (Boston, MA: Springer) p 389
- [13] Kamal M 2006 *Radiat. Eff. Defects Solids* **161** 189
- [14] Otsuka K and Ren X 2002 *Mater. Sci. Forum* **394–395** 177
- [15] Ren X and Otsuka K 2000 *Mater. Sci. Forum* **327–328** 429
- [16] Ahlers M 1986 *Prog. Mater. Sci.* **30** 135
- [17] Frick C P, Ortega A M, Tyber J, Maksound A El M, Maier H J, Liu Y *et al* 2005 *Mater. Sci. Eng. A* **34–49** 405

- [18] Mazzer E M, Gargarella P, Kiminami C S, Bolfarini C, Cava R D and Galano M 2017 *J. Mater. Res.* **3165–3174** 32
- [19] Liu Y 2010 in *Shape memory alloys* H R Chen (ed) (New York: Nova Science Publishers Inc) p 361
- [20] Raju T N and Sampath V 2011 *Trans. IITM* **64** 165
- [21] Raju T N and Sampath V 2011 *J. Mater. Eng. Perform.* **20** 767
- [22] Raju T N 2013 PhD thesis *Synthesis and characterization of Cu–Al–Fe shape memory alloys indian institute of technology* (Chennai, India: Indian Institute of Technology, Madras)
- [23] Kumar P, Jain A K, Hussain S, Pandey A and Dasgupta R 2015 *Materia (Rio. J)* **20** 284
- [24] Recarte V, Perez-Saez R B, Bocanegra E H, No M L and Juan J S 1999 *Mater. Sci. Eng. A* **273–275** 380
- [25] Zhang X and Liu Q 2018 *Intermetallics* **92** 108
- [26] Guilemany J M and Gil F J 1990 *Mater. Lett.* **10** 145
- [27] Sathish S, Mallik U S and Raju T N 2014 *J. Miner. Mater. Char. Eng.* **2** 71
- [28] Barbarino S, Flores E I S, Ajaj R M, Dayyani I and Friswell M I 2014 *Smart Mater. Struct.* **23** 1
- [29] Yujun B, Chengweil L, Guili G and Longwei Y 2001 *Chin. Sci. Bull.* **46** 1837
- [30] Bujoreanu L G, Craus M L, Stanciu S and Dia V 2000 *Mater. Sci. Technol.* **16** 612
- [31] Wield D V and Gillam E 1977 *Acta Metall.* **25** 725
- [32] Dutkiewicz J, Chandrasekaran M and Cesari E 1993 *Scr. Mater.* **29** 19
- [33] Miura S, Maeda S and Nakanishi N 1975 *Scr. Metall.* **9** 675